

See discussions, stats, and author profiles for this publication at: <https://www.researchgate.net/publication/5441059>

Charge-Coupled Device Operated in a Time-Delayed Integration Mode as an Approach to High-Throughput Flow-Based Single Molecule Analysis

ARTICLE in ANALYTICAL CHEMISTRY · JUNE 2008

Impact Factor: 5.64 · DOI: 10.1021/ac800447x · Source: PubMed

CITATIONS

16

READS

26

2 AUTHORS:



Jason Emory

Pfeiffer University

7 PUBLICATIONS 120 CITATIONS

SEE PROFILE



Steven Soper

Louisiana State University

201 PUBLICATIONS 5,509 CITATIONS

SEE PROFILE

Charge-Coupled Device Operated in a Time-Delayed Integration Mode as an Approach to High-Throughput Flow-Based Single Molecule Analysis

Jason M. Emory and Steven A. Soper*

Department of Chemistry, Louisiana State University, Department of Mechanical Engineering, and Center for BioModular Multi-Scale Systems, Louisiana State University, Baton Rouge, Louisiana 70803

Single molecule detection (SMD) readouts are particularly attractive for assays geared toward high-throughput processing, because they can potentially reduce assay time by eliminating various processing steps. Unfortunately, most flow-based SMD experiments have generated low throughputs due primarily to the fact that they are configured in single assay formats. The use of a charge-coupled device (CCD) with flow-based SMD can image multiple single molecule assays simultaneously to realize high-throughput processing capabilities. We present, for the first time, the ability to simultaneously track and detect single molecules in multiple microfluidic channels by employing a CCD camera operated in time-delayed integration (TDI) mode as a means for increasing the throughput of any single molecule measurement. As an example of the technology, we have configured a CCD to operate in a TDI mode to detect single double-stranded DNA molecules (λ and pBR322) labeled with an intercalating dye (TOTO-3) in a series of microfluidic channels poised on a poly(methyl methacrylate), PMMA, chip. A laser beam was launched into the side of the chip, which irradiated a series of fluidic channels (eight) with the resulting fluorescence imaged onto a CCD. Using this system, we were able to identify single DNA molecules based on the fluorescence burst intensity arising from differences in the extent of dye labeling associated with the DNA molecule length. The CCD/TDI approach allowed increasing sample throughput by a factor of 8 compared to a single-assay SMD experiment. A sampling throughput of 276 molecules s^{-1} per channel and 2208 molecules s^{-1} for an eight channel microfluidic system was demonstrated. Operated in its full capacity, this multichannel format was projected to yield a sample throughput of 1.7×10^7 molecules s^{-1} , which represents a 170-fold improvement over previously reported single molecule sampling rates.

Processing of biochemical/chemical information in high-throughput formats is becoming a necessity in systems targeted for a variety of applications, such as genome sequencing, molecular diagnostics, and drug discovery to name a few. High rates of

information throughput can be accomplished by building systems that process many samples in parallel, increase the multiplexing capability of the assay, reduce processing time, or use a combination of the aforementioned approaches. The ability to process large amounts of biochemical/chemical information has been realized through the evolution of several novel technologies, such as capillary array electrophoresis,^{1–3} high density plate readers⁴ and micro-total analysis systems (μ -TAS).^{5,6} The use of μ -TAS has significantly enhanced throughput capabilities for many applications due to characteristics inherent in this technology, such as decreased analysis times, full automation of the sample processing pipeline, and the ability to configure processing units in a highly parallel fashion.⁷

Single molecule detection (SMD) is another enabler that can assist in realizing high-throughput processing due to its ability to eliminate sample processing steps in multistep assays (reduce assay time) and the short readout times required for each single molecule event. For example, Wabuyele et al. demonstrated the ability to detect single nucleotide polymorphisms (SNPs) from genomic DNA in less than 5 min using single-pair FRET.⁸ Reductions in processing times were realized by eliminating the overhead time associated with PCR amplification of the target DNA being interrogated.

For flow-based SMD experiments in which the single molecule events are transported either hydrodynamically or electrokinetically through a fixed interrogation (sampling) zone, the sample throughput (ST) can be calculated from

$$ST = (SE)(DE)(DR)(DC) \quad (1)$$

where SE represents the percentage of molecules that are sampled during the experimental run, DR is the delivery rate of molecules

- (1) Mathies, R. A.; Huang, X. C. *Nature* **1992**, 359, 167–169.
- (2) Huang, X. H. C.; Quesada, M. A.; Mathies, R. A. *Anal. Chem.* **1992**, 64, 967–972.
- (3) Lu, X. D.; Yeung, E. S. *Appl. Spectrosc.* **1995**, 49, 605–609.
- (4) Huang, K. S.; Mark, D.; Ganderberger, F. U. In *Measuring Biological Responses with Automated Microscopy*; Elsevier: Amsterdam, The Netherlands, 2006; Vol. 414, pp 589–600.
- (5) Blom, N.; Fetting, J. C.; Koch, J.; Ludi, H.; Manz, A.; Widmer, H. M. *Sens. Actuators, B* **1991**, 5, 75–78.
- (6) Dittrich, P. S.; Manz, A. *Anal. Bioanal. Chem.* **2005**, 382, 1771–1782.
- (7) Soper, S. A.; Ford, S. M.; Qi, S.; McCarley, R. L.; Kelly, K.; Murphy, M. C. *Anal. Chem.* **2000**, 72, 642A–651A.
- (8) Wabuyele, M. B.; Farquar, H.; Stryjewski, W.; Hammer, R. P.; Soper, S. A.; Cheng, Y. W.; Barany, F. J. *Am. Chem. Soc.* **2003**, 125, 6937–6945.

* To whom correspondence should be addressed.

into the sampling volume, DC is the readout duty cycle, and DE is the detection efficiency. SE is calculated from

$$SE = \frac{\pi\omega_0^2}{dw} \quad (2)$$

where ω_0 is the $1/e^2$ laser beam waist (cm) and d and w are the depth and width (cm) of the flow cell. DR can be calculated using

$$DR = F_v C_b \quad (3)$$

where F_v represents the volume flow rate ($\text{cm}^3 \text{s}^{-1}$) and C_b is the molecular concentration (molecules cm^{-3}). DE is basically the percentage of molecules detected above a threshold value, which is selected to minimize the number of false positives generated during the experiment.

As can be seen from eq 1, increasing the laser spot size, the volume flow rate, or the concentration of the input sample can increase ST. However, these parameters must be balanced by the requirements for achieving high signal-to-noise ratios (SNR) in the single molecule measurement⁹ and generating high confidence that the signals monitored during readout are those emanating from single molecule events.¹⁰ For example, in the case of fluorescence single molecule detection with the excitation laser possessing a $1/e^2$ beam waist of $7 \mu\text{m}$ (probe volume $\sim 1 \text{ pL}$), a square bore flow tube with a $100 \mu\text{m}$ width ($SE = 0.015$), $F_v = 2 \times 10^{-5} \text{ cm}^3 \text{s}^{-1}$, and a concentration of $1 \times 10^8 \text{ molecules cm}^{-3}$ ($DR = 2000 \text{ s}^{-1}$), a ST of only $30 \text{ molecules s}^{-1}$ would be realized. The value for F_v was selected based on the condition that the transit time must be approximately equal to the bleaching lifetime of the fluorophore when excited at optical saturation to produce optimal SNR in the single molecule measurement,⁵ and the concentration was chosen to minimize the probability of double occupancy within the sampling (probe) volume.

Confocal setups that are commonly used in many SMD experiments focus the laser beam to a diffraction-limited area within a sampling channel and have a pinhole filter in the secondary image plane of the relay objective to spatially reject light from outside the focal volume, which can improve the SNR in the single molecule measurement. While this setup ensures high DE, it results in low SE. An alternative approach would be to maximize the SE to improve ST by overfilling the sampling channel with the laser excitation beam and removing the pinhole filter.

A format for increasing single molecule ST is to operate the reader in a multichannel configuration, in which samples are dynamically passed through a series of parallel fluidic channels. The resulting fluorescence would be imaged onto a series of detectors with the increase in throughput directly related to the number of channels being interrogated. A charge-coupled device (CCD) provides a platform to image multiple flow-type SMD experiments simultaneously, which can have a profound influence on the SMD ST. For example, van Orden et al. described a CCD-based single molecule flow cytometer system in which the effluent from a square-bore tube was imaged onto a 1152×1240 pixel

CCD camera operated in the snapshot mode.¹¹ The authors used the system to perform single DNA fragment sizing and were able to demonstrate an increase in ST from $100 \text{ fragments s}^{-1}$ using a single element detector to $2000 \text{ fragments s}^{-1}$ using the CCD approach. Unfortunately, the camera was operated in the snapshot mode, which significantly reduced the duty cycle of the measurement (duty cycle = t_{int}/T , where t_{int} is the signal accumulation time, and $T = t_{\text{int}} + t_{\text{rd}}$, where t_{rd} is the CCD readout time).

Another operational mode of the CCD is time-delayed integration (TDI), which has been used in astronomy to track weak light emitting objects by adjusting the parallel shift rate of the camera to match the rate of movement of the emitting object. Sweedler and co-workers first applied this CCD mode to an electrophoretic separation in a capillary.¹² They discovered that the advantages of TDI over the snapshot mode were reductions in the amount of data produced, increases in the integration times, better duty cycles, and reduced read noise.¹³ Recently, Hesse and co-workers were able to demonstrate the ability to use the TDI mode for the CCD in a single molecule imaging experiment, in which fluorescently labeled lipid molecules embedded in bilayer membranes were interrogated. The scanning speed over the surface to be imaged was matched with the parallel shift rate of the CCD camera. The authors were able to demonstrate the ability to image a $5 \text{ mm} \times 5 \text{ mm}$ area in $\sim 11 \text{ min}$.¹⁴

A full description of the TDI operational mode is given in the Supporting Information.^{12,15} Briefly, the parallel shift of the CCD is synchronized with the movement of a light emitting entity as it moves across the field-of-view of the fluorescence microscope so that the photogenerated signal is collected into the same potential well of the CCD array. The SNR enhancement for the TDI-mode scales with $N^{1/2}$, where N is the number of rows in the CCD camera used in the parallel shift.

In this report, we present for the first time a multichannel system for flow-based single molecule measurements using a CCD camera operated in a TDI mode as a means for increasing the ST of any single molecule measurement. We adapted the CCD to operate in the TDI mode to track single double-stranded DNA molecules (λ and pBR322) labeled with an intercalating dye (TOTO-3) in a series of microfluidic channels poised on a PMMA-based microchip. A laser beam was launched into the side of the chip, which irradiated a series of fluidic channels (eight) with the resulting fluorescence imaged onto the CCD.

EXPERIMENTAL DETAILS

Optical Setup. The optical system used for the flow-based multichannel single molecule measurements is shown in Figure 1a. Excitation was provided by a Sanyo DL5038-21 635 nm laser diode (Thorlabs, Newton, NJ) that was mounted in a temperature control unit (TCLDM9, Thorlabs). The laser output was passed

(9) Mathies, R. A.; Peck, K.; Stryer, L. *Anal. Chem.* **1990**, *62*, 1786–1791.
(10) Nie, S. M.; Chiu, D. T.; Zare, R. N. *Anal. Chem.* **1995**, *67*, 2849–2857.

(11) Van Orden, A.; Keller, R. A.; Ambrose, W. P. *Anal. Chem.* **2000**, *72*, 37–41.
(12) Sweedler, J. V.; Shear, J. B.; Fishman, H. A.; Zare, R. N.; Scheller, R. H. *Anal. Chem.* **1991**, *63*, 496–502.
(13) Hanley, Q. S.; Earle, C. W.; Pennebaker, F. M.; Madden, S. P.; Denton, M. B. *Anal. Chem.* **1996**, *68*, A661–A667.
(14) Hesse, J.; Jacak, J.; Kasper, M.; Regl, G.; Eichberger, T.; Winklmayr, M.; Aberger, F.; Sonnleitner, M.; Schlapak, R.; Howorka, S.; Muresan, L.; Frischauf, A. M.; Schutz, G. J. *Genome Res.* **2006**, *16*, 1041–1045.
(15) Karger, A. E.; Weiss, R.; Gesteland, R. F. *Anal. Chem.* **1993**, *65*, 1785–1793.

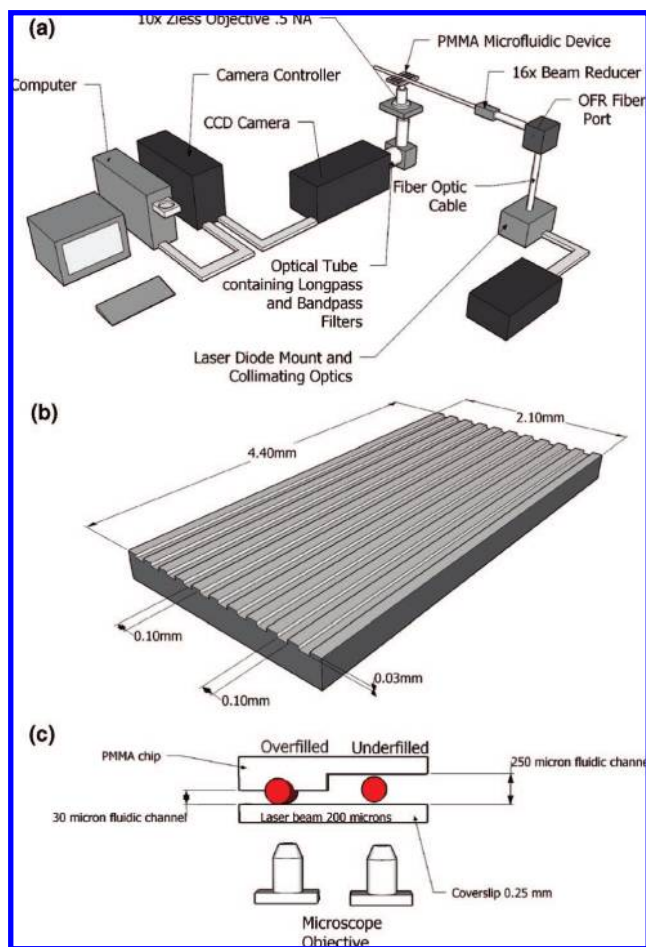


Figure 1. (a) Instrumental arrangement for the high-throughput, multichannel single molecule detection system using a PMMA microfluidic device and a CCD camera operated in a TDI mode. (b) Dimensions of the PMMA chip used for multichannel detection. (c) Horizontal illumination of the PMMA microfluidic device using either an overfilled or underfilled design of the fluidic channels with the laser beam. The overfilled design used 30 μm deep channels while the underfilled design used 250 μm deep channels. Both designs were irradiated by a 200 μm diameter ($1/e^2$) laser beam with 10 mW of average laser power.

through a 635 nm laser line filter (XL37, Omega Optical, Brattleboro, VT) before being collimated with an aspheric lens (C230TM-B, Thorlabs). The laser beam was then directed through a Newport 20 \times , 0.40 NA objective that focused the laser beam into a single mode fiber optic cable (P1-630A-FC-2, Thorlabs), which was used to produce a circular beam from the elliptical output of the diode laser. The fiber output was launched into an OFR fiber port (PAF-X-11- λ , OFR, Caldwell, NJ) to produce a collimated beam with a diameter of 2.4 mm. A beam expander was used in the reverse mode to reduce the beam diameter to 200 μm ($1/e^2$). The beam reducer consisted of a plano-concave lens with a focal length of -6.0 mm and a plano-convex lens with a focal length of 100.0 mm (LC2969-A, AC254-100-A1, Thorlabs). The collimated beam was then launched into the side of a PMMA microchip.

The fluorescence emission was collected with a low magnification, high numerical aperture objective (Fluar 10 \times , 0.50 NA, Carl Zeiss, Germany) from the bottom side of the PMMA chip and orthogonal to the laser propagation axis. The collected light was directed through an optical tube, which contained a long-pass filter

(650 nm long-pass, FEL0650, Thorlabs) and a laser rejection filter (XB23, Omega Optical). A Roper Scientific (Trenton, NJ) Spec-10 charge-coupled device camera was used to transduce the fluorescence photons and was placed at the secondary image plane of the collection objective. The CCD camera was thermoelectrically cooled to -90 $^{\circ}\text{C}$ and contained a 1 MHz digital converter for fast data acquisition. The CCD possessed 20 μm pixels and was configured in a 1340 \times 100 back-illuminated format. The net velocity of the single molecules through the field-of-view was matched with the parallel shift of the CCD. The strip images of the TDI process were examined after each run to determine if the parallel shift matched the net velocity of the single molecules. If the timing was mismatched, the molecular images appeared as streaks across the strip image whereas if they were matched, the molecules appeared as discrete spots on the TDI image (see Figure S1 in Supporting Information).

Microfluidic Chips. The microfluidic devices were fabricated following previously published procedures for producing a mold master and using this master for subsequent hot embossing and coverslip annealing (see Supporting Information for additional details on the fabrication and chip assembly process).¹⁶ The microchips consisted of a series of microchannels that were 100 μm wide with a pitch of 100 μm and common sample/waste reservoirs situated at the termini of all fluidic channels (see Figure 1b). The depth of these channels was designed to be either 250 or 30 μm . Following assembly, the laser entry side of the PMMA chip was polished on a granite stone (TRU-Stone Technologies, Waite Park, MN) with Bueller-METII silicon carbide of Grit 400/P800 and then Grit 600/P1200. Finally, the laser input side was polished with a felt disk using a polycrystalline diamond suspension of 9 μm followed by a 1 μm suspension to give an optically transparent entry port for the excitation beam.

Chemicals and Materials. Borate buffers were prepared by dissolving the desired amount of sodium borate (Sigma Chemical) into nanopure water secured from a Barnstead NANOpure Infinity System (model D8991, Dubuque, IA). The pH was adjusted by the addition of concentrated NaOH or HCl. The buffer was diluted to a final concentration of 50 mM and filtered with a 0.2 μm filter before use. Fluorescent reagents used in these experiments consisted of AlexaFluor 647, crimson fluorescent FluoSpheres (diameter = 1.0 μm), and TOTO-3, which were purchased from Molecular Probes (Eugene, OR). An amount of 1 μg of λ -DNA (48.5 kbp) and pBR322 (4.3 kbp), obtained from New England Biomedical Research, were diluted in 25 mM borate buffer (pH 9.1). The bis-intercalating dye, TOTO-3, was added at a 5:1 molar ratio (bp/dye). The samples were diluted in borate buffer to yield the desired concentration.

TDI Timing. Optimization of TDI timing was performed using crimson fluorescent FluoSpheres diluted in 25 mM borate buffer. The beads were loaded into the common sample reservoir of the PMMA chip and moved through the microfluidic channels by electrokinetic pumping ($E = 250$ V/cm) using a high-voltage power supply (Caberria Industries, model 3002, Meriden, CT). The shift rate was adjusted by changing the integration time until the shift rate matched the net velocity of the spheres in the fluidic channels. In the case of the single molecule DNA measurements,

(16) Hupert, M. L.; Guy, W. J.; Llopis, S. D.; Shadpour, H.; Rani, S.; Nikitopoulos, D. E.; Soper, S. A. *Microfluid. Nanofluid.* **2007**, *3*, 1–11.

the shift rate of the CCD was matched to the apparent mobility of the stained DNA through inspection of the CCD images.

A histogram of the photon burst intensity of the individual DNA molecules versus number of events was generated. A Gaussian curve was fit to the distributions to give the average photon burst size per molecule and the standard deviation for each distribution, which could be related to the size of the DNA fragment due to the stoichiometric staining by the bis-intercalating dye.^{11,17}

RESULTS AND DISCUSSION

Optical Illumination of the Multichannel Architecture.

There are basically two strategies in which to illuminate a series of microchannels for multichannel excitation: illumination from the side of the chip using a properly shaped beam or using a laser line generated from a cylindrical lens irradiating the entire array of channels from the top of the chip. As noted by Mathies et al., multichannel illumination with a laser line requires high laser powers to operate near optical saturation to produce optimal SNR in a single molecule measurement, which can produce high background levels due to scattering from the substrate/solution interfaces and generate large probe volumes.¹⁸ Side-illumination using a collinear beam can reduce the high laser power requirements to achieve optimal irradiance and also provides less scattering at the substrate/solution interfaces.¹⁹ Typically, the laser beam would underfill the channel to reduce specularly scattered radiation generated at the substrate/solution interface. Using the laser beam shaping optics in this study, we were able to produce a collimated beam with a waist ($1/e^2$) of $200\ \mu\text{m}$ over the imaging area requiring an $\sim 250\ \mu\text{m}$ deep channel to create such a geometry (see Figure 1c). The numerical aperture of the relay objective was determined to give a depth of focus of $\sim 6.6\ \mu\text{m}$. Therefore, some molecules would produce “blurred” or weak images in the CCD TDI strip images if a $250\ \mu\text{m}$ deep channel was used because many of the molecules would be outside the relay objective’s depth of focus. This configuration would also produce a low SE, because the width of the beam is less than the channel depth. In order to avoid this, we also investigated the use of an overfilled (see Figure 1c) geometry, in which the $200\ \mu\text{m}$ beam was launched into channels that were only $30\ \mu\text{m}$ deep to keep most of the single molecule events within the depth of focus of the relay optic and also every molecule traversing through the channel would be sampled (i.e., high SE).

We compared the scattering patterns generated from both the overfilled design (channel depth of $30\ \mu\text{m}$) and the underfilled design (channel depth of $250\ \mu\text{m}$) with constant laser diameter and power ($200\ \mu\text{m}$ $1/e^2$ waist and 10 mW, respectively). Figure 2 shows CCD images collected from these two illumination formats using buffer-filled channels (six channels were evaluated). As can be seen, the absolute scattering intensity from the overfilled geometry was approximately 56% that of the underfilled configuration (mean = 2297 for overfilled; mean = 3887 counts for underfilled geometry) due to attenuation of the beam when

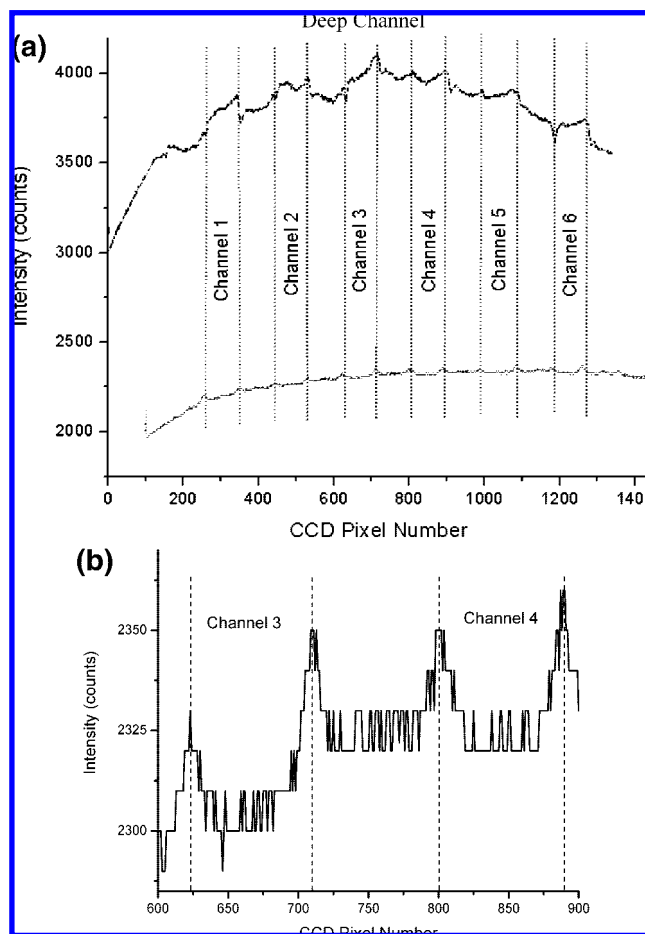


Figure 2. (a) Scattering profiles measured from $250\ \mu\text{m}$ deep and $30\ \mu\text{m}$ deep channels. An expanded view of the scattering profile produced from the $30\ \mu\text{m}$ deep chip is shown in part b. The chips were illuminated with a 10 mW laser (635 nm) and a beam waist ($1/e^2$) of $200\ \mu\text{m}$. The channels were filled with borate buffer (pH = 9.1).

launched into the shallower channels. However, the degree of beam attenuation was not directly related to the decrease in channel depth (30 versus $250\ \mu\text{m}$, 12%) most likely due to the higher scattering backgrounds generated for the shallower channels. Close inspection of the trace shown for the $30\ \mu\text{m}$ deep channels (see Figure 2b) indicated that the intensity changed only minimally across the array (RSD = 2% for overfilled and RSD = 3% for underfilled).

The overfilled horizontal illumination format was further evaluated by filling the parallel fluidic channels with AlexaFluor 647 dye and monitoring the emission using the CCD camera operated in the snapshot mode. The average fluorescence emission intensity (background corrected) from eight fluidic channels was found to be 2159 counts with a standard deviation of 38 counts (RSD = 1.7%). With an input beam waist of $200\ \mu\text{m}$, a cross sectional area of $4.4 \times 10^{-4}\ \text{cm}^2$ was calculated, which produced an irradiance of $7.3 \times 10^{19}\ \text{photons cm}^{-2}\ \text{s}^{-1}$ (average laser power = 10 mW) for both the under-filled and overfilled illumination geometries. The fluorescence emission scales linearly with the irradiance until the molecule’s excited-state is saturated ($k_{a(\text{sat})}$), which occurs when $k_{a(\text{sat})} \sim 1/\tau_f$, where τ_f is the fluorescence lifetime. Zander and co-workers found that for a typical molecular fluorescence lifetime of 10 ns and an absorption cross section of

(17) Wabuyele, M. B.; Ford, S. M.; Stryjowski, W.; Barrow, J.; Soper, S. A. *Electrophoresis* **2001**, *22*, 3939–3948.

(18) Woolley, A. T.; Sensabaugh, G. F.; Mathies, R. A. *Anal. Chem.* **1997**, *69*, 2181–2186.

(19) Chen, D. H.; Peterson, M. D.; Brumley, R. L.; Giddings, M. C.; Buxton, E. C.; Westphall, M.; Smith, L.; Smith, L. M. *Anal. Chem.* **1995**, *67*, 3405–3411.

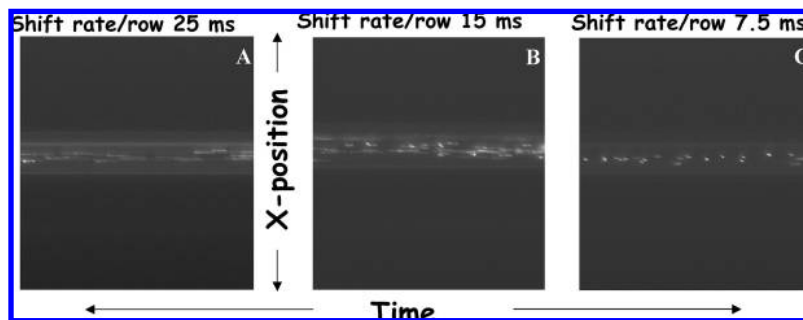


Figure 3. The effects of the parallel shift rate on the TDI images of fluorescent microspheres. The parallel shift rate of the CCD was incrementally changed: (a) 25 ms, (b) 15 ms, and (c) 7.5 ms. The images were accumulated using the fluorescent microspheres excited at 635 nm and electrokinetically pumped using $E = 250$ V/cm.

1.6×10^{-16} cm², optical saturation occurs at an irradiance of approximately 6.2×10^{23} photons cm⁻² s⁻¹.²⁰ Therefore, we are approximately 4 orders of magnitude below optical saturation. Reductions in the beam waist and/or increases in the laser power could further improve the SNR in these single molecule measurements. In the remainder of this work, we adopted a horizontal illumination format with the microchannel depth (30 μ m) close to the depth of field of the objective and overfilled the channels to increase the SE.

TDI Timing Optimization. TDI testing was performed by filling the fluidic microchannels with fluorescent microspheres such that the particle density resulted in a single particle occupancy probability of 0.1 in order to reduce the probability of double occupancy. The single particle occupancy probability, P_v , can be calculated from the product of the detection volume, D_v (L), and the particle density, C_p (particles L⁻¹). In the present case, D_v is not the same as the excitation volume (0.6 nL), which is defined by the $1/e^2$ laser beam waist (200 μ m) and the physical dimensions of the fluidic channel (30 μ m \times 100 μ m) but is instead defined by the total magnification of the optical system (10 \times) and the size of the individual pixels of the CCD camera (20 μ m), producing a D_v of 0.12 pL. Therefore, the particle density for these experiments was selected at 8.3×10^{11} particles L⁻¹.

The TDI timing was optimized by matching the parallel shift rate of the CCD camera with the linear rate of travel of the fluorescent microspheres (see Figure 3) with successful matching determined by observing nonstreaked images of the beads. The image of Figure 3a shows long faint streaks, which indicated the timing of the TDI shift rate and bead velocity were mismatched. The image of Figure 3b demonstrated better timing between the bead linear velocity and shift rate due to decreases in the lengths of the streaks shown in the image. As can be seen from the data of Figure 3c, nonstreaked images were produced when the CCD parallel shift was set to a rate of 7.5 ms per row, which corresponded to a bead linear velocity of 0.27 cm/s and an apparent mobility of 1.06×10^{-3} cm²/V s. The advantage of electrophoretic pumping as opposed to hydrodynamic pumping is that the flow is pluglike and, as such, the mobility is constant irrespective of the location along the axial direction of the fluidic path. In the case of a mixture of DNA molecules with different sizes, the free solution electrophoretic mobility of DNA is independent of length, and therefore, the same shift rate can be

used to interrogate samples comprised of different sized DNAs due to the DNA's free draining behavior.²¹

Comparison of TDI versus Snapshot Modes for CCD Operation. We made a rigorous comparison of the performance metrics of TDI versus snapshot modes of operation for the CCD in single molecule experiments using the fluorescent microbeads. The results of these studies can be found in the Supporting Information. Briefly, the TDI mode produced a single particle SNR of 150 compared to 7 for the snapshot mode when the CCD integration time was less than the particle's transit time. In addition, the duty cycle was 100% for TDI and only 65% for the snapshot mode.

Detection of Single DNA Molecules Using TDI. The TDI optimization for the detection of single DNA molecules labeled with an intercalating dye (TOTO-3) was carried out using horizontal illumination with the CCD camera operated in the TDI mode using λ -DNA and pBR322 as model targets. TOTO-3 binds stoichiometrically to double-stranded DNA, and therefore, the single molecule burst size can be related to the length (in bp) of the DNA molecule being interrogated.¹¹ The samples were diluted to ~ 1 and 10 pM for λ -DNA and pBR322, respectively. The DNAs were electrokinetically pumped through the microfluidic channels by setting $E = 125$ V/cm and the fluorescence tracked by adjusting the TDI shift rate to 8 ms per shift. A typical single DNA molecule TDI image for an eight-channel measurement is shown in Figure 4a. The peak pixel intensity of each molecular event was identified and recorded from several runs. The data was then plotted as a histogram of molecular events versus burst intensity with the resulting distributions fit to Gaussian functions to secure the mean and standard deviations of the photon bursts (see Figure 4b). The mean background (913 units) and standard deviation of the noise (13) was used to plot a Gaussian distribution of the background noise. A threshold level of 3σ above the average background (952 units) was employed to minimize errors due to false positives and thus, only events exceeding this level were scored as events. The lower amplitude burst distribution was found to possess a mean of 974 units with a standard deviation of 17, which we attributed to the smaller pBR322 DNAs. The second distribution provided a mean of 1268 units with a standard deviation of 23, which was assigned to λ -DNA due to its larger size compared to pBR322. In addition, because pBR322 DNA was

(21) Stellwagen, N. C.; Gelfi, C.; Righetti, P. G. *Biopolymers* **1997**, *42*, 687–703.

(22) Yang, R.; Wang, W. J.; Soper, S. A. *Appl. Phys. Lett.* **2005**, *86*.

(20) Zander, C. *Fresenius J. Anal. Chem.* **2000**, *366*, 745–751.

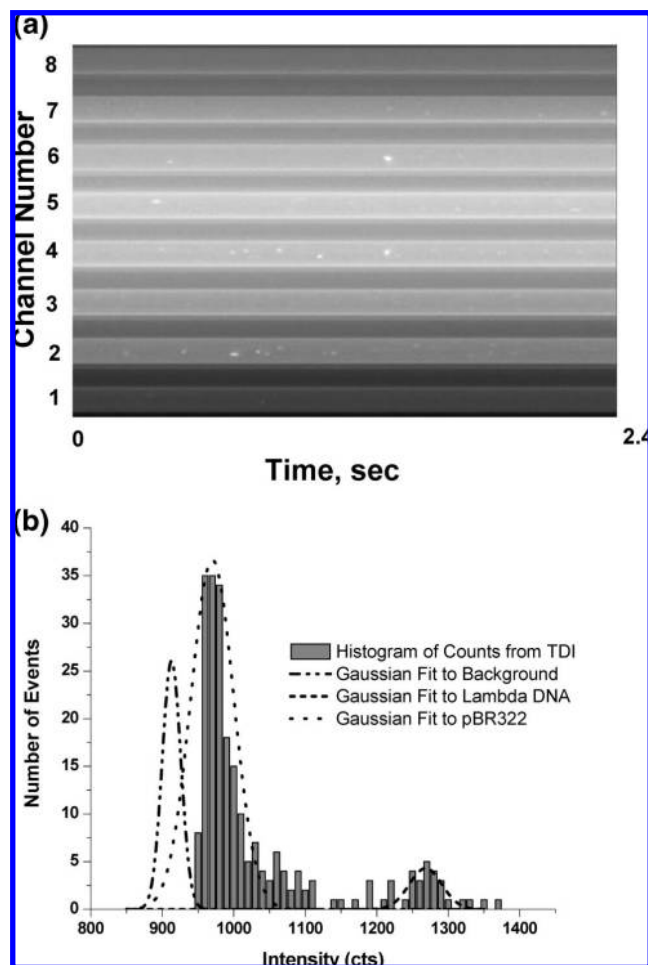


Figure 4. (a) TDI image of λ -DNA and pBR322 DNAs traveling electrokinetically through eight microfluidic channels with an orthogonally positioned Gaussian laser beam (25 mM borate buffer pH 9.1; shift rate 8 ms; $E = 125$ V/cm; 10 mW; $\lambda_{\text{ex}} = 635$ nm). (b) Histograms of the peak intensities versus number of events from TDI images shown in part a. The histograms were fit to Gaussian functions from which the mean burst amplitude and standard deviations were derived (mean = 1268, standard deviation = 23 for λ -DNA and mean = 974, standard deviation = 17 for pBR322). A Gaussian curve of the noise was also plotted to determine the detection threshold level of 952. The intensity in the images was truncated below the threshold level of ~ 952 pixel counts.

loaded into the device at a 10-fold higher copy number compared to λ -DNA, the number of events for this distribution was consistent with the higher number concentration of pBR322. The ratio of the mean burst intensity was 5.7, which is in close agreement to the length ratio of the two DNAs (λ -DNA/pBR322 = 11.3). The background corrected counts for pBR322 was determined to be 61 and with a background noise standard deviation of 13, the SNR for pBR322 in these experiments is 4.7. Because of truncation of the data below 952 CCD units, the pBR322 distribution is skewed and the Gaussian fit should be viewed as provisional in this case.

High-Throughput DNA Detection Using TDI. The TDI detection system was then set up to demonstrate the ability to process large numbers of single molecule events by increasing the DNA concentration and also increasing the delivery rate. A solution of 1.0×10^7 molecules cm^{-3} of λ -DNA labeled with TOTO-3 was loaded into an eight-channel microfluidic chip. The parallel shift rate in this case was set to the maximum value (1

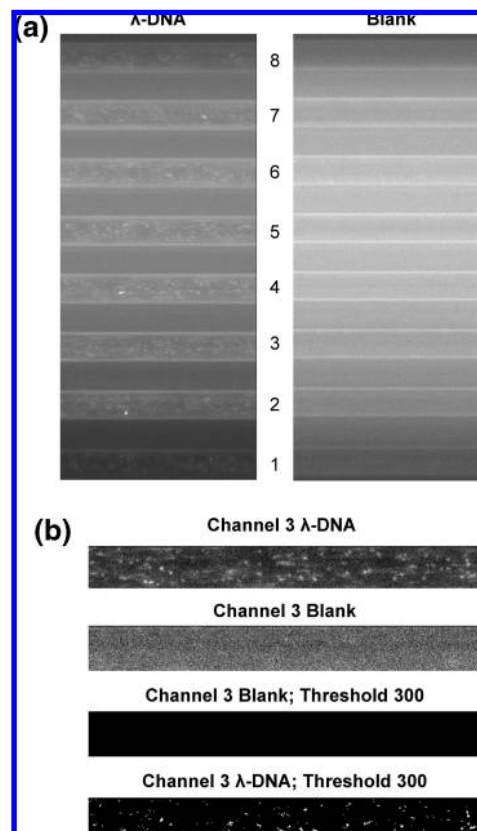


Figure 5. (a) TDI image of λ -DNA labeled with TOTO-3 and a blank TDI image (25 mM borate buffer, pH 9.1; shift rate of 1 ms^{-1} ; $E = 425$ V/cm; 10 mW; $\lambda_{\text{ex}} = 635$ nm). (b) Enlarged images of channel 3 from part a after the average background were subtracted at 3σ above the mean. At this threshold level of 300, the blank had no counts but the λ -DNA TDI image produced 138 individual molecular events in the image.

ms^{-1}), and the electrical field was adjusted to give correct timing ($E = 425$ V/cm). The TDI images from a buffer blank and sample from these runs are shown in Figure 5a. The average background was subtracted from the images to set a threshold condition to minimize false positive signals and individual events were then counted from enlarged frames (see Figure 5b). The ST for this data set was determined to be $276 \text{ molecules s}^{-1}$ per channel corresponding to $2208 \text{ molecules s}^{-1}$ for imaging the entire eight channel microfluidic chip.

We can further improve both the SNR and the ST for the CCD-based TDI mode of operation for single molecule detection using eq 1 as a guide. For example, reducing the excitation beam waist to $\sim 5 \mu\text{m}$ will increase the irradiance by 1600 improving the SNR in the single molecule measurements. Also, reductions in the channel depth from 30 to $\sim 1 \mu\text{m}$ will improve the SE and reduce the effective probe volume, hence further reducing background signal. The DR of molecules entering a single channel observation zone in this case depends on the maximum parallel shift rate of the CCD camera, which is hardware limited and sets the maximum volume flow rate (assuming a microchannel cross-sectional area of $1 \times 10^{-6} \text{ cm}^2$) to $1.06 \times 10^{-6} \text{ cm}^3/\text{s}$. If we assume that the probability of single molecule occupancy is set at 0.1 (probability of double occupancy is 0.01), the concentration (C_b) that can be used for a probe volume of $4 \times 10^{-12} \text{ cm}^3$ (probe volume defined by the CCD pixel size, $20 \mu\text{m}$, the total magnifica-

tion of the optical system, 10 \times , and a channel depth of 1 μm), the maximum concentration allowed by these conditions would be 2.5×10^{10} molecules cm^{-3} . Therefore, an acceptable DR would be 2.6×10^4 molecules s^{-1} . Assuming a DE of 1.0, the ST for a single channel is calculated to be approximately 26 000 molecules s^{-1} (duty cycle, DC, for our TDI CCD readout mode is 1.0). Because the system in the present case used eight parallel channels, the total system ST is 208 000 molecules s^{-1} . In addition, we have not fully utilized the imaging capacity of the CCD camera in the present system in terms of the number of channels that could be interrogated simultaneously. The CCD used in these experiments possessed 1340 pixels for channel imaging. Diffraction limited resolution is approximately $\lambda/2$ indicating that the channel and interchannel spacing could be reduced to ~ 350 nm in order to optically resolve each experiment, which means our CCD could image 670 channels. This would yield a theoretical ST of 1.7×10^7 molecules s^{-1} . Van Orden and co-workers suggested that their snapshot CCD single molecule system could detect $\sim 100\,000$ fragments s^{-1} , which would suggest that our experimental system could provide an ~ 170 -fold higher ST.¹¹

CONCLUSION

The ability to simultaneously track and detect flowing single molecules in multiple microfluidic channels by employing a CCD camera operated in a TDI mode was demonstrated using double-stranded DNA labeled with an intercalating dye as the model. TDI was shown to offer some attractive characteristics in terms of single molecule readout. For example, the TDI mode of operation provided a DC near 100% and favorable SNR for single molecule detection as compared to a snapshot mode of operation where the DC was only 65% and provided a lower single molecule SNR (SNR = 150 for TDI and SNR = 7 for snapshot; see Table S1). In addition, the imaging capacity of the CCD can offer some unique

opportunities in terms of ST. For microchannels geometrically configured in a diffraction limited architecture, the system could effectively image ~ 670 channels, providing a single molecule ST of $> 10^7$ molecules s^{-1} .

Using the size of the DNA interrogated in this study and the molar ratio of dye-to-DNA base pairs, we calculated that the load of dye per DNA molecule was approximately 9700 for λ -DNA and 860 for pBR322 DNA. The results depicted in Figure 4b produced a SNR for pBR322 of 4.7, indicating that the present system does not display single fluorophore sensitivity in its current format. Improvements in the SNR for single-fluorophore detection can be realized by increasing the irradiance. Reduction of the laser beam waist and channel depth to more closely match the depth of focus for the optics (1 μm), the use of a higher laser power (100 mW), and the integration of micro-optics, such as free-standing SU-8 converging lenses for slight focusing of the laser beam in the center of the channels,²² would provide the necessary increase in the irradiance to approach optical saturation.

ACKNOWLEDGMENT

The authors would like to thank the National Institutes of Health (Grants EB002115, EB6639), the National Science Foundation (Grant EPS-0346411), and the Louisiana Board of Regents for financial support of this work.

SUPPORTING INFORMATION AVAILABLE

Additional information as noted in text. This material is available free of charge via the Internet at <http://pubs.acs.org>.

Received for review March 3, 2008. Accepted March 5, 2008.

AC800447X